Estimation of Rack Swing Torque for Rack and Pinion Steering Gear

T. KOBAYASHI H. SHIBATA

In this paper, we discuss rack swing torque of rack and pinion steering gears considering friction during rack and pinion gear meshing without backlash and present a theory able to estimate rack swing torque based on consideration of rack and pinion gear meshing normal force, frictional force between tooth surfaces, spring force, frictional force from the rack guide, etc. In addition, based on this theory, we tested rack and pinion gear parameters designed to minimize rack swing torque. The experimental results show that the rack swing angle is improved compared with that of the current product and consequently that the proposed theory for estimating rack swing torque is effective.

***Key Words**: rack and pinion gear, rack swing torque, gear meshing, frictional force*

1. Introduction

The steering system used predominantly in passenger cars today is the rack and pinion type[1)], in regard to which the rack and pinion (R&P) meshing quality significantly affects steering system vibration, noise and feeling. The R&P also plays the major role of directly transmitting road condition information from the tires to the driver.

The steering system R&P, depending on engine room packaging requirements, often must be designed such that the rack and pinion axes do not meet perpendicularly, as shown in **Fig. 1**. Because of this skewed engagement, meshing action gives rise to sliding in a helical direction, which creates torque tending to rotate the cylindrical rack (the steering system "rack bar"). Since the steering system structure allows such rack bar rotation to be suppressed only by the meshing R&P tooth surfaces, it is thought that rack bar rotation generated by such meshing influences meshing quality.

However, because the steering wheel is turned in the right and left directions, the rack bar rotates in both the clockwise and counterclockwise directions and rocks back and forth together with steering wheel right and left turning. Such rack bar rotation is referred to as "swing," and the torque and angle of this rotation are referred to as "swing torque" and "swing angle (degree)," respectively.

If only the meshing of the skewed type R&P is considered, it is possible to discuss tooth profile and the gear meshing process by the general theory of gears[2)], as in the case of crossed helical gears. However, although, in regard to steering system R&Ps, there have been theoretical studies on R&P meshing friction and mechanical efficiency[3)] as well as projects to evaluate R&P meshing and torque characteristics by modeling[4), 5)], no research literature could be found concerning rack swing resulting from R&P meshing. Until now there hasn't been theory taking rack swing into account that can be used to support specification optimization in the steering system R&D design process, and therefore a large amount of experimental data has had to be relied on in order to improve vibration and noise or evaluate feeling. Experiments have had to be carried out repeatedly, increasing the cost and lead-time of new product development, and furthermore it has been difficult to find optimal specifications. It therefore has been imperative to establish analytical theory for steering system R&P designing that takes into account rack swing.

The authors analyzed the characteristics of steering system R&P meshing using gear meshing theory and derived a theoretical equation to obtain the contact line at the time of simultaneous meshing of both tooth flanks

Fig. 1 Rack and pinion steering gear

(no backlash). We also studied the gear tooth friction generated from gear meshing and derived an equation to compute the relative sliding velocity between tooth flanks during the meshing process (in both tooth trace and tooth depth directions).

Moreover, using the meshing line and the relative sliding velocity, we have established a theory for estimating the rack swing torque based on such factors as the force exerted on the rack due to meshing and the force exerted on the rack through the rack guide peculiar to the steering.

Finally, we have attempted to create a design in which swing torque is minimized based on the theory obtained in this research and validated the results. This paper describes these results.

2. Coordinate Systems for Steering System R&P Meshing Analysis

2. 1 Definition of Coordinate Systems

In discussing R&P meshing theory of R&P, the pinion and rack coordinate systems must first be defined. An absolute coordinate system having the same axis as the pinion axis is defined to be the pinion coordinate system, and another absolute coordinate system having the same axis as the rack axis is defined as the rack coordinate system.

As shown in **Fig. 2**, the pinion coordinate system S_p (o-x, y, z) consists of the xy plane, which is perpendicular to the pinion axis including the shortest distance between the offset rack axis line and pinion axis line, the x-axis, which corresponds to the line of shortest distance between both axes, and the direction toward the rack being positive. The y-axis is defined on the plane perpendicular to the pinion axis based on the right hand system. Also, the intersection of the xy plane and the pinion axis line is defined as the origin o, and the pinion axis line as the z-axis.

On the other hand, the rack coordinate system S_r (O-X, Y, Z) consists of the XY plane, which is the rack axis plane including the shortest distance between the offset rack axis line and the pinion axis line, and the X-axis representing the shortest distance between these axes with its direction corresponding to the X-axis direction. The intersection of the X-axis and the rack axis line is defined as the origin O, and the rack axis line as the Y-axis. Also, the direction of the Y-axis is so defined that the skewing angle (stagger angle) between the Y-axis and y-axis becomes sharp, and the direction of the Z-axis is defined by the plane perpendicular to the rack axis based on the right hand system.

Figure 2 (a) shows the overall positional relationship, and **Fig. 2** (b) and (c) show the YZ and XZ planes, respectively.

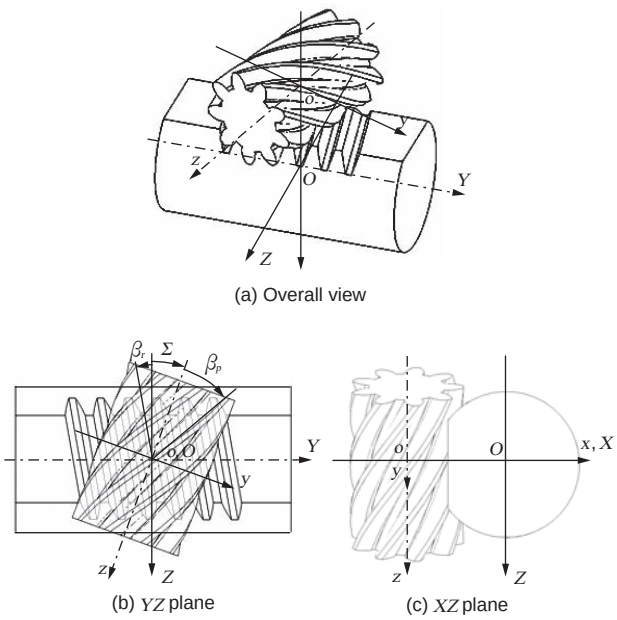

Fig. 2 Definition of coordinate systems

When there exists an angle difference (stagger angle) between the two axes, and supposing that the helix angles of the pinion and rack to be β_p, and β_r, respectively, the angle between the pinion axis line and the perpendicular line of the rack axis becomes the axis angle Σ (= β_p + β_r). The direction of each angle is defined as positive when twisted rightward in **Fig. 2** (b).

The relationship between the pinion and the rack coordinates is such that they are rotated by axis angle Σ (-Σ) around the x (X) axis with their origins being separated on the x (X) axis by the axis-to-axis distance a.

2. 2 Transformation of Coordinate System

The positional relationship between pinion coordinate system S_p (o-x, y, z) and rack coordinate system S_r (O-X, Y, Z) as defined in the previous subsection is represented by the x (X) axis, which is the same for both coordinate systems. One system is rotated by Σ (-Σ) around the x (X) axis and moved by distance ±a thereon.

For instance, when an arbitrary position in space is expressed by the use of the pinion coordinate system S_p, its position vector $\boldsymbol{K}_p$ is given by the following equation:

$$\boldsymbol{K}_p = \{x,\ \ y,\ \ z\}^T \tag{1}$$

On the other hand, if expressed by the rack coordinate system S_r, its position vector $\boldsymbol{K}_r$ is given by the following equation:

$$\boldsymbol{K}_r = \{X,\ \ Y,\ \ Z\}^T \tag{2}$$

Using the positional relationship between the two coordinate systems, the two vectors expressed in the above equations (1) and (2) can be mutually transformed as follows:

$$\left.\begin{aligned} \boldsymbol{K}_r &= M_x^{-\Sigma}\boldsymbol{K}_p - \boldsymbol{a} \\ \boldsymbol{K}_p &= M_x^{\Sigma}\boldsymbol{K}_r + \boldsymbol{a} \end{aligned}\right\} \quad (3)$$

The transformation matrix and position vector in the equation (3) are as follows:

$$M_x^{\mp\Sigma} = \begin{bmatrix} 1 & 0 & 0 \\ 0 & \cos\Sigma & \mu\sin\Sigma \\ 0 & \pm\sin\Sigma & \cos\Sigma \end{bmatrix}, \quad \boldsymbol{a} = \{a,\ 0,\ 0\}^T$$

3. Derivation of Theoretical Equation for Estimating Rack Swing Torque

3. 1 Definitions of Load Exerted on Rack and Friction

In order to derive rack swing torque T, which is generated along with the process of R&P meshing, the force exerted on the rack is first considered.

The rack is subject to not only the tooth flank normal load due to meshing with the pinion and the friction load accompanying the relative sliding between the rack and pinion teeth, but also the rack radial load exerted by the rack for the purpose of maintaining constant contact between both teeth peculiar to the steering; the sliding friction load between the rack guide and the rack; external loads from the tires, etc.

Figure 3 shows the above loads received by the rack and swing torque generated on the rack. **Figure 3** (a) shows the rack axis plane (XY plane), and **Fig. 3** (b) shows the plane perpendicular to the rack axis (XZ plane). **Table 1** shows the definitions of the loads, friction coefficients, etc.

Among these loads, the normal load received from the pinion tooth flank is divided into that from the pinion's right tooth flank and that from the left tooth flank, each being defined as P_R and P_L, assuming that in each case a certain constant load is exerted on the unit length of the meshing line. Also, as shown in **Fig. 4**, as P_R and P_L are exerted on the tooth flank perpendicularly, their directional vectors $\boldsymbol{e}_{rR}$ and $\boldsymbol{e}_{rL}$, if expressed in the rack coordinate system, can be given in the following equation using the tooth normal pressure angle α_n:

$$\left.\begin{aligned} \boldsymbol{e}_{rR} &= \{\sin\alpha_n,\ \cos\alpha_n\cos\beta_r,\ \cos\alpha_n\sin\beta_r\}^T \\ \boldsymbol{e}_{rL} &= \{\sin\alpha_n,\ -\cos\alpha_n\cos\beta_r,\ -\cos\alpha_n\sin\beta_r\}^T \end{aligned}\right\} \quad (4)$$

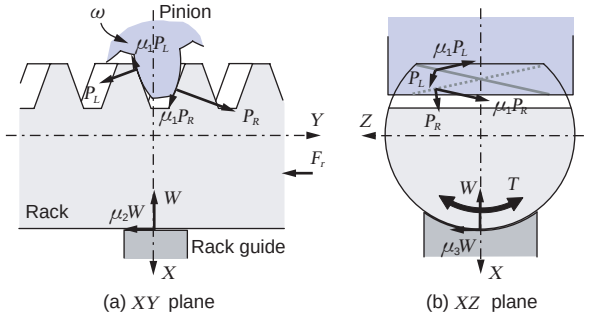

Fig. 3 Loads exerted on rack

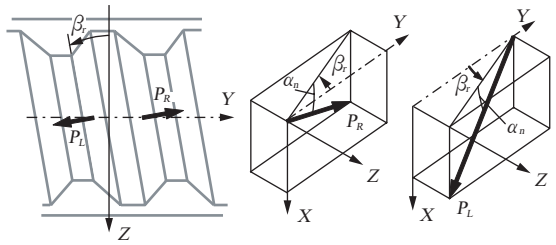

Fig. 4 Directions of load exertion on rack tooth

Table 1 Definitions of rack loads and friction coefficients

Pinion angular velocity	ω
Load from right tooth flank*1	P_R
Load from left tooth flank*1	P_L
Tooth flank friction coefficient	μ_1
External force on rack	F_r
Rack guide load	W
Rack guide friction coefficient in rack axial direction	μ_2
Rack guide friction coefficient in rack circumferential direction	μ_3
Rack swing torque	T

*1: Load per unit length of meshing line

3. 2 Direction of Relative Sliding Velocity in Tooth Meshing

3. 2. 1 Derivation of Relative Sliding Velocity in Helical Direction

In the case the R&P axial angle is $\Sigma \neq 0$, because the rack and pinion have different helix angles, the relative sliding generated from R&P meshing is not only in the tooth depth direction but also in the helical direction. In this subsection, the relative sliding velocity in the helical direction is derived.

Assuming that, on the pinion coordinate system S_p, an arbitrary meshing point K on the tooth flank has coordinates (x, y, z) and that angular velocity of the pinion is ω, the pinion peripheral velocity at the meshing point is expressed as follows:

$$v_{pT} = \sqrt{x^2 + y^2}\,\omega \quad (5)$$

As shown in **Fig. 5**, the components of the pinion peripheral velocity in the tooth normal direction can be obtained from equation (5) as follows:

$$v_{pN} = \sqrt{x^2 + y^2}\,\omega \cos\alpha' \tag{6}$$

In equation (6), α' represents the pressure angle at meshing point K on the plane perpendicular to the pinion axis. Also, because of an involute tooth profile, the following equation stands:

$$\sqrt{x^2 + y^2}\cos\alpha' = r\cos\alpha_t \tag{7}$$

In equation (7), r stands for the pitch circle radius, and α_t represents the pressure angle in the pitch circle on the plane perpendicular to the pinion axis. Here, by substituting equation (7) for equation (6), the components of pinion peripheral velocity in the tooth normal direction can be rewritten as follows:

$$v_{pN} = r\,\omega\cos\alpha_t \tag{8}$$

Consequently, the component (y axis component) on the rack axis plane (YZ plane) derived from the pinion peripheral velocity as shown in **Fig. 5** can be obtained as follows:

$$v_{pNy} = \frac{v_{pN}}{\cos\alpha_t} = r\,\omega \tag{9}$$

As seen in equation (9), the component in the YZ plane as obtained from the pinion peripheral velocity is constant irrespective of the meshing position. Furthermore, if the vector $\boldsymbol{v}_{pNy}$ of v_{pNy} is expressed by the pinion coordinate system, the following equation stands:

$$\boldsymbol{v}_{pNy} = \{0,\ r\,\omega,\ 0\}^T \tag{10}$$

The component $\boldsymbol{v}_p$ which is the component on the ZX plane obtained from the pinion peripheral velocity and expressed on the rack coordinate system, can be given as follows, utilizing coordinate transformation equation (3):

$$\boldsymbol{v}_p = M_x^{-\Sigma}\boldsymbol{v}_{pNy} = \{0,\ r\,\omega\cos\Sigma,\ r\,\omega\sin\Sigma\}^T \tag{11}$$

Incidentally, on the planes parallel to both the pinion axis line and the rack axis line, there exist components of the pinion peripheral velocity $\boldsymbol{v}_p$ and the rack movement velocity to the axial direction $\boldsymbol{v}_r$ as shown in **Fig. 6**. This is because when the R&P is meshing, the tooth flanks are in contact, i.e. the velocity $\boldsymbol{v}_N$ on the shared plane of the rack and the pinion (the plane perpendicular to the tooth) is equal, so that the relational equation between $\boldsymbol{v}_p$ and $\boldsymbol{v}_r$ can be derived as follows:

$$\left.\begin{aligned} v_N &= v_p\cos\beta_p = v_r\cos\beta_r \\ v_r &= v_p\frac{\cos\beta_p}{\cos\beta_r} = r\,\omega\frac{\cos\beta_p}{\cos\beta_r} \end{aligned}\right\} \tag{12}$$

Therefore, the sliding velocity on the R&P meshing teeth, as shown in **Fig. 6**, can be given by the following equation based on equations (11) and (12):

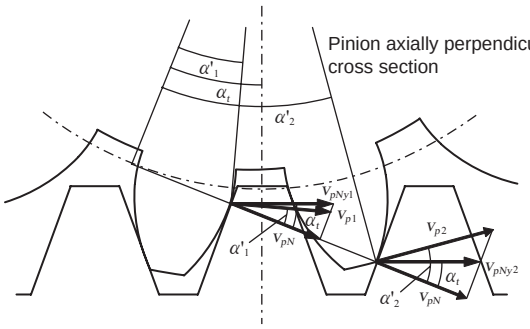

Fig. 5 Pinion peripheral velocity at meshing point

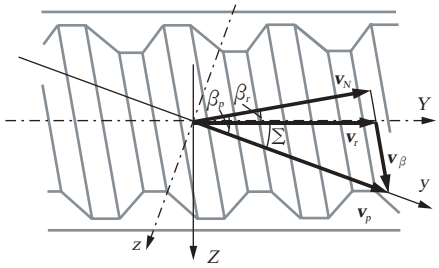

Fig. 6 Relative sliding velocity in helical direction

$$\boldsymbol{v}_\beta = \boldsymbol{v}_p - \boldsymbol{v}_r = \left\{0,\ r\,\omega\left(\cos\Sigma - \frac{\cos\beta_p}{\cos\beta_r}\right),\ r\,\omega\sin\Sigma\right\}^T \tag{13}$$

By calculating the magnitude of the vector expressed in equation (13), the relative sliding velocity in the tooth trace direction can be obtained as follows:

$$v_\beta = r\,\omega\frac{\sin\Sigma}{\cos\beta_r} \tag{14}$$

3. 2. 2 Derivation of Relative Sliding Velocity in Tooth Depth Direction

In the tooth depth direction of a gear having involute tooth profile, relative sliding occurs between the meshing of two teeth because they are rotating while sliding due to their different meshing length of both teeth.

When two gear teeth mesh with each other, the actual tooth sliding friction in the tooth depth direction can be obtained based on the teeth relative sliding ratio[6]. Sliding velocity v_α in the tooth depth direction at an arbitrary point K (x, y, z) on the tooth meshing surface can be given in the following equation:

$$v_\alpha = u\sqrt{x^2 + y^2}\,\omega \tag{15}$$

Where, u represents the tooth relative sliding ratio, which can be obtained as follows[6]:

$$u = 1 - \frac{\tan\alpha_t}{\tan\alpha'}$$

Supposing that the radius of the pinion shaft at an arbitrary meshing point K is r', the following equation can be obtained:

$$r' = \sqrt{x^2 + y^2} \tag{16}$$

By substituting equation (16) for equation (15), the relative sliding velocity in the tooth depth direction can be expressed as follows:

$$v_\alpha = ur'\omega \tag{17}$$

Also, the relative sliding velocity in the tooth depth direction can be represented by the vector using the pinion coordinate system as follows:

$$\boldsymbol{v}_\alpha = ur'\omega \{\sin\alpha_t, -\cos\alpha_t, 0\}^T \tag{18}$$

3. 2. 3 Derivation of Aggregate Relative Sliding Velocity on Tooth Meshing

From equations (14) and (18), when meshing of both teeth occurs, aggregate relative sliding velocity $\boldsymbol{v}_s$ can be obtained on the rack coordinate system, as follows:

$$\begin{aligned}\boldsymbol{v}_s &= M_x^{-\Sigma}\boldsymbol{v}_\alpha + \boldsymbol{v}_\beta \\ &= \omega\begin{Bmatrix} ur'\sin\alpha_t \\ -ur'\cos\alpha_t\cos\Sigma + r\left(\cos\Sigma - \dfrac{\cos\beta_p}{\cos\beta_r}\right) \\ -ur'\cos\alpha_t\sin\Sigma + r\sin\Sigma \end{Bmatrix}\end{aligned} \tag{19}$$

Where, as the relative sliding velocity in the tooth depth direction is expressed in the pinion coordinate system, the velocity is transformed into the rack coordinate system by the use of the coordinate transformation matrix shown in equation (3).

Also, its unit direction vector $\boldsymbol{e}_s$ can be given by the following equation:

$$\boldsymbol{e}_s = \frac{\boldsymbol{v}_s}{|\boldsymbol{v}_s|} \tag{20}$$

3. 3 Load Exerted on Tooth Flank Including Tooth Relative Sliding Friction

From equations (4) and (20), the unit direction vector of the load received from the right flank of the pinion tooth, including the sliding friction, can be given in the following equation:

$$\boldsymbol{e}_{fR} = \frac{P_R\boldsymbol{e}_{pR} - \mu_1 P_R\boldsymbol{e}_s}{|P_R\boldsymbol{e}_{pR} - \mu_1 P_R\boldsymbol{e}_s|} = \frac{\boldsymbol{e}_{pR} - \mu_1\boldsymbol{e}_s}{|\boldsymbol{e}_{pR} - \mu_1\boldsymbol{e}_s|} \tag{21}$$

Where, μ_1 represents the tooth friction coefficient. Therefore, its load $\boldsymbol{f}_R$ can be given in the following equation:

$$\boldsymbol{f}_R = P_R\boldsymbol{e}_{fR} \tag{22}$$

Then, using equation (22), the total load received from the right tooth flank of the pinion is obtained.

As described above, since equation (22) provides the load per unit length of the meshing line, the total load received from the right tooth flank of the pinion can be obtained by the following equation, whereby using minute length dl_R, the load on each meshing line on the simultaneously meshing teeth are summed up.

$$\sum\int \boldsymbol{f}_R\, dl_R = \sum\int P_R\boldsymbol{e}_{fR}\, dl_R \tag{23}$$

Similarly, by equations (4) and (20), the unit direction vector of the load received from the left tooth flank of the pinion, including the sliding friction, can be given in the following equation:

$$\boldsymbol{e}_{fL} = \frac{P_L\boldsymbol{e}_{pL} - \mu_1 P_L\boldsymbol{e}_s}{|P_L\boldsymbol{e}_{pL} - \mu_1 P_L\boldsymbol{e}_s|} = \frac{\boldsymbol{e}_{pL} - \mu_1\boldsymbol{e}_s}{|\boldsymbol{e}_{pL} - \mu_1\boldsymbol{e}_s|} \tag{24}$$

Then, its load $\boldsymbol{f}_L$ can be given in the following equation:

$$\boldsymbol{f}_L = P_L\boldsymbol{e}_{fL} \tag{25}$$

Again, using equation (25), the total load received from the left tooth flank of the pinion is calculated. As in the case of the right tooth flank, the total load received from the left tooth flank of the pinion can be given in the following equation using minute length dl_L for the load on each meshing line:

$$\sum\int \boldsymbol{f}_L\, dl_L = \sum\int P_L\boldsymbol{e}_{fL}\, dl_L \tag{26}$$

3. 4 Balance of Forces on Rack

As the load received from the both pinion tooth flanks including sliding friction has been obtained in equations (23) and (26) derived in the previous subsection, here in this subsection, we will derive the force balance equation on the rack to obtain loads P_R and P_L per unit length of the meshing line received from the two pinion tooth flanks.

The force exerted on the rack includes, in addition to the loads on the tooth obtained by equations (23) and (26), external load $\boldsymbol{F}_r$ in the rack axis direction, radial load $\boldsymbol{W}$ from the rack guide, and axial load $\mu_2\boldsymbol{W}$ due to the rack guide friction. The balance of these forces is expressed as follows:

$$\boldsymbol{F}_r + \boldsymbol{W} + \mu_2\boldsymbol{W} = \sum\int \boldsymbol{f}_R dl_R + \sum\int \boldsymbol{f}_L dl_L \tag{27}$$

Where, the rack guide friction is assumed to act in the direction opposite to the pinion rotation.

Incidentally, in order that the load exerted on the rack be discussed in terms of the rack axial direction as well as the direction perpendicular to the rack axis and the pinion axis (i.e. perpendicular direction parallel to the x- and X-axes), the unit direction vector indicated in equation (21) and (24) will be expressed as follows:

$$\left.\begin{aligned}\boldsymbol{e}_{fR} &= \{e_{fXR}, e_{fYR}, e_{fZR}\}^T \\ \boldsymbol{e}_{fL} &= \{e_{fXL}, e_{fYL}, e_{fZL}\}^T\end{aligned}\right\} \tag{28}$$

Also, if the positive direction of each load is defined by the arrowed direction in **Fig. 3**, the following equation can be derived from the balance in the rack axial direction:

$$F_r + \frac{\omega}{|\omega|}\mu_2 W = \sum\int P_R e_{fYR} dl_R + \sum\int P_L e_{fYL} dl_L \quad (29)$$

On the other hand, the following equation stands from the balance in the directions perpendicular to the rack axis and the pinion axis:

$$W = \sum\int P_R e_{fXR} dl_R + \sum\int P_L e_{fXL} dl_L \quad (30)$$

Here, since P_R and P_L are defined, respectively, as constant per unit length of the meshing line, they can be obtained as follows using equations (29) and (30):

$$P_R = \frac{W\sum\int e_{fYL} dl_L - (F_r + \frac{\omega}{|\omega|}\mu_2 W)\sum\int e_{fXL} dl_L}{\sum\int e_{fXR} dl_R \sum\int e_{fYL} dl_L - \sum\int e_{fYR} dl_R \sum\int e_{fXL} dl_L} \quad (31)$$

$$P_L = \frac{W\sum\int e_{fYR} dl_R - (F_r + \frac{\omega}{|\omega|}\mu_2 W)\sum\int e_{fXR} dl_R}{\sum\int e_{fXL} dl_L \sum\int e_{fYR} dl_R - \sum\int e_{fYL} dl_L \sum\int e_{fXR} dl_R} \quad (32)$$

Since it is generally considered that $P_R \geqq 0$, and $P_L \geqq 0$, in the case of $P_R < 0$ or $P_L < 0$ in equations (31) and (32), the rack guide is considered to have yielded, and can be obtained as follows: When $P_L < 0$ in equation (29), assuming $P_L = 0$, P_R is expressed as follows:

$$P_R = \frac{F_r + \frac{\omega}{|\omega|}\mu_2 W}{\sum\int e_{fYR} dl_R} \quad (33)$$

Similarly, when $P_R < 0$ in equation (29), assuming $P_R = 0$, P_L is expressed as follows:

$$P_L = \frac{F_r + \frac{\omega}{|\omega|}\mu_2 W}{\sum\int e_{fYL} dl_L} \quad (34)$$

3. 5 Derivation of Rack Swing Torque

Swing torque is derived from the moment around the rack axis. As the load component exerted on the plane perpendicular to the rack axis (XZ plane) is to be discussed, loads $\boldsymbol{f}_R$ and $\boldsymbol{f}_L$ received from the two pinion flanks, as obtained earlier, are expressed as follows:

$$\left.\begin{aligned} \boldsymbol{f}_R &= \{f_{XR},\ f_{YR},\ f_{ZR}\}^T \\ \boldsymbol{f}_L &= \{f_{XL},\ f_{YL},\ f_{ZL}\}^T \end{aligned}\right\} \quad (35)$$

First, the moment around the rack axis due to the load received from the right flank of the pinion is calculated. As shown in **Fig. 7**, supposing point (Z_R, X_R) on the meshing line, the load component is expressed as follows:

$$\sqrt{f_{XR}^2 + f_{ZR}^2} \quad (36)$$

Also, the equation for the line of the load component passing through the meshing points is given in the following equation:

$$X - X_R = \frac{f_{XR}}{f_{ZR}}(Z - Z_R) \quad (37)$$

Furthermore, distance d_R between the load component and the center of the rack axis O (0, 0, 0) is expressed as follows:

$$d_R = \frac{|f_{ZR} X_R - f_{XR} Z_R|}{\sqrt{f_{XR}^2 + f_{ZR}^2}} \quad (38)$$

Therefore, the moment T_R around rack axis due to the load received from the right flank of the pinion is given in the following equation derived from equations (36) and (38):

$$\begin{aligned} T_R &= \sum\int \sqrt{f_{XR}^2 + f_{ZR}^2}\, dl_R \cdot d_R \\ &= \sum\int \sqrt{f_{XR}^2 + f_{ZR}^2}\, dl_R \cdot \frac{|f_{ZR} X_R - f_{XR} Z_R|}{\sqrt{f_{XR}^2 + f_{ZR}^2}} \\ &= \sum\int |f_{ZR} X_R - f_{XR} Z_R|\, dl_R \end{aligned} \quad (39)$$

Incidentally, the direction of equation (39) for giving the moment T_R around the rack axis can be determined as follows: In the case of $X = 0$ in equation (37), suppose:

(i) If $-\frac{f_{ZR}}{f_{XR}} X_R + Z_R \geq 0$ then, $|f_{ZR} X_R - f_{XR} Z_R|\, dl_R$

(ii) If $-\frac{f_{ZR}}{f_{XR}} X_R + Z_R < 0$ then, $-|f_{ZR} X_R - f_{XR} Z_R|\, dl_R$

In this way, the sum of the moment around the rack axis due to load received from the right pinion flank can be obtained.

Similarly, moment T_L around the rack axis due to load received from the left pinion tooth flank, also, can be obtained by substituting suffix L for the left tooth flank for the suffix R for the right tooth flank in the following equation:

$$\begin{aligned} T_L &= \sum\int \sqrt{f_{XL}^2 + f_{ZL}^2}\, dl_L \cdot d_L \\ &= \sum\int \sqrt{f_{XL}^2 + f_{ZL}^2}\, dl_L \cdot \frac{|f_{ZL} X_L - f_{XL} Z_L|}{\sqrt{f_{XL}^2 + f_{ZL}^2}} \\ &= \sum\int |f_{ZL} X_L - f_{XL} Z_L|\, dl_L \end{aligned} \quad (40)$$

Putting equations (39) and (40) together, the moment around the rack axis shown in **Fig. 7**, i.e. rack swing torque T, is expressed as follows.

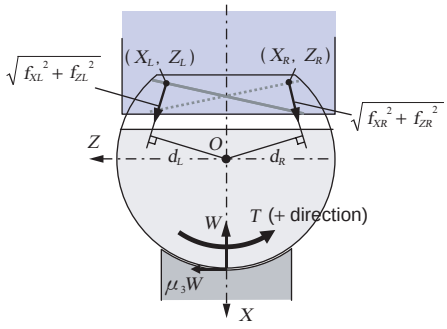

Fig. 7 Derivation of rack swing torque

$$T = T_R + T_L - \frac{T_R + T_L}{|T_R + T_L|}\mu_3 W \cdot R_r \quad (41)$$

In equation (41), R_r represents the radius of the rack bar shown in **Fig. 7**, indicating that the moment due to the rack guide friction works in such direction that the absolute value of swing torque T becomes smaller.

Thus, the theory of rack swing torque in the steering system due to R&P meshing has been established as intended in this research.

4. Design Trial for Minimizing Steering Rack Swing Torque due to R&P Meshing

Utilizing the theory described above, the rack swing torque due to R&P meshing of the current R&P for steering as shown in **Fig. 8** (a) was estimated. The results are shown as the black curve in **Fig. 9**, where the horizontal axis represents the rotational angle of the pinion, and the vertical axis shows the rack swing torque.

As seen in the figure, the process of R&P meshing brings about rack swing torque, whose direction changes in accordance with the left/right change of pinion rotation. In addition, fluctuation of rack swing torque arises during meshing of one pitch, which is considered to be caused by variation of the sliding velocity between the teeth at the meshing position in the R&P. In short, the maximum value and the variation range of the swing torque generated on the rack can be estimated by use of the theory derived in **Section 3**.

Furthermore, in order to improve steering feeling, a design for minimizing rack swing torque caused by R&P meshing has been tried, using the theory in the **Section 3**. While keeping installation and strength conditions, such as R&P shaft angle, center line distance, specific stroke and rack diameter, nearly unchanged, minimum value T_{min} of the rack swing torque has been calculated with module (m), helix angle (β) and addendum modification coefficient (ζ) as the parameters.

$$T_{\min} \equiv \min \{T(m, \beta_p, \beta_r, \xi)\} \quad (42)$$

Figure 8 (b) shows the R&P trial product produced based on data of each parameter that can provide the minimum rack swing torque using equation (42). Similarly, the rack swing torque due to the R&P meshing as shown in **Fig. 8** (b) was estimated using the theory in the **Section 3**, with the result as shown in the red curve in **Fig. 9**.

As seen in the figure, the maximum value and variation range of the rack swing torque of the trial R&P product with the minimized swing torque are lower than those of the current product. These comparison results are shown in **Fig. 10**. **Figure 10** (a) shows comparison results of the swing torque maximum values, and **Fig. 10** (b) shows

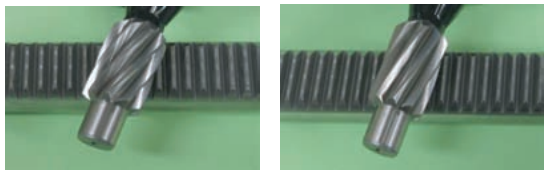

(a) Current product (b) Trial product

Fig. 8 Rack and pinion products

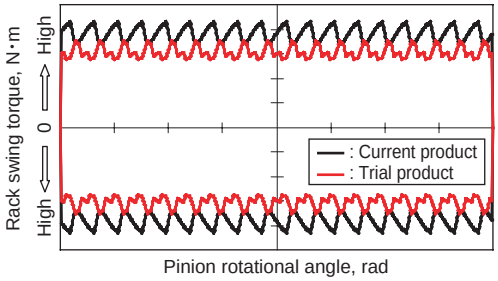

Fig. 9 Results of rack swing torque calculation

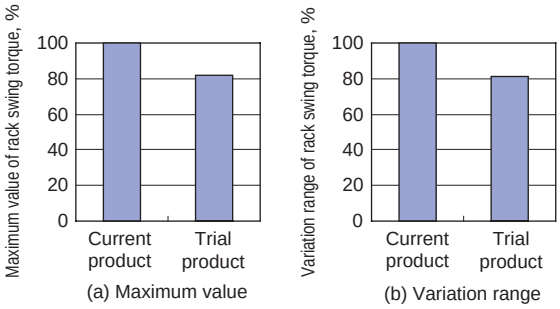

Fig. 10 Results of trial product and current product comparison

those of the swing torque variation range. The horizontal axes show the current product and trial product, and the vertical axes represent the swing torque maximum values and variation range (normalized by the values of current product, %).

Also, in order to verify the effect of minimization of the swing torque obtained by the theoretical estimation, the rack swing angle of the current product shown in **Fig. 8** (a) and the trial product shown in **Fig. 8** (b) were each measured using the test machine shown in **Fig. 11**. As the test machine is equipped with a rack guide simulation mechanism, the rack swing angle was measured during pinion rotation under the conditions of no backlash and low loading.

The measured rack swing angle is shown in **Fig. 12**. In the figure, the black curve shows the rack swing angle for the current product, and the red curve shows that for the trial product. The horizontal axis shows the pinion rotational angle, and the vertical axis shows the rack swing angle.

Although variation of the rack swing angle within one meshing pitch cannot be distinguished because of very

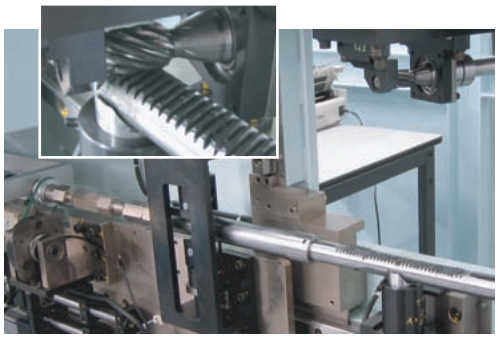

Fig. 11 Gear meshing test machine

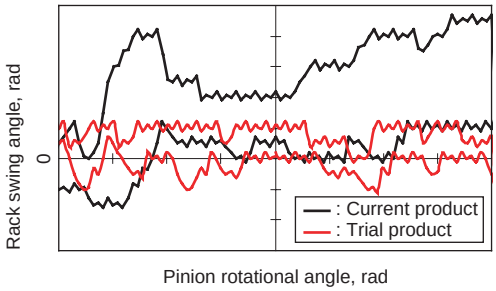

Fig. 12 Results of rack swing angle measurement

small measured values of the swing angle, it is evident from the figure that for the trial product with minimized swing torque, the swing angle has been changed less than that of the current product, indirectly verifying the superiority of the trial product based on theoretical estimation. In other words, the effectiveness of the theory in **Section 3** has been confirmed.

5. Conclusions

Taking the R&P for steering, we have studied the gear tooth friction taking place in simultaneous meshing on both tooth flanks without backlash and discussed the rack swing torque generated in such gear meshing. The results of this study are summarized as follows:

(1) A theoretical equation to estimate the relative sliding velocity (both in tooth depth and tooth trace directions) generated in the process of meshing has been derived. Using this, the tooth flank friction force has been derived.

(2) Based on studies of the tooth flank friction force generated due to the meshing of gears, the tooth normal force exerted on the rack due to the meshing, the force exerted on the rack from the rack guide peculiar to steering, etc., a theory for estimating rack swing torque has been established.

(3) An attempt was made to design an R&P with specifications minimizing swing torque, and then a trial R&P product was prepared and evaluated. The trial product showed improvement in the rack swing angle compared to the current product. Thus the effectiveness of this theoretical approach has been verified.

References

1) Society of Automotive Engineers of Japan: Jidousya Gizyutu Handbook (Vol. 5 Design (Chassis)), (2005).
2) F. L. Litvin: Gear Geometry and Applied Theory, Prentice-Hall, Inc, (1994).
3) S. J. Wou; T. D. Oste & J. Baxter: Modelling of Mesh Friction and Mechanical Efficiency of Rack and Pinion Steering Design, SAE, (2001).
4) Naresh Dayanand Kamble & Subir K. Saha: Effect of Pinion Profile Modification on Rack and Pinion Steering Gear, SAE, (2005).
5) Naresh Dayanand Kamble & Subir K. Saha: Evaluation of Torque Characteristics of Rack and Pinion Steering Gear Using ADAMS Model, SAE, (2005).
6) M. Senba: Haguruma (Vol. 1), Nikkan Kogyo Shimbun Ltd., (1971).


T. KOBAYASHI* H. SHIBATA**

* *Mechatronic Systems R&D Dept., Research & Development Center, PhD*
** *Mechatronic Systems R&D Dept., Research & Development Center*